Electrochemistry of Vitamin B_{12}. 5. Cyanocobalamins

D. Lexa,[1a] J. M. Savéant,*[1a] and J. Zickler[1b]

Contribution from the Laboratoire d'Electrochimie de L'Université de Paris VII, 75221 Paris Cedex 05, France, and the Laboratoire de Biophysique du Muséum d'Histoire Naturelle, 75005 Paris, France. *Received July 25, 1979*

Abstract: Cyanide is taken as a representative example illustrating the general problem of how a strong ligand may influence the oxidoreduction patterns of vitamin B_{12}. The thermodynamics of the system is derived from the results of long time range spectroelectrochemical experiments. The resulting $E°$–log [CN^-] diagram provides a complete description of the thermodynamic stability of the various B_{12} forms as a function of potential and cyanide concentration. The description of the reaction pathways followed under dynamic conditions and how they change with the main external parameters—CN^- concentration and magnitude of the electron flux—is derived from a kinetic analysis carried out in the context of cyclic voltammetry. The interaction of CN^- with cobalt results in a strong tendency toward direct two-electron reduction of Co(III) into Co(I). This problem is discussed for equilibrium as well as for dynamic conditions. The formation of cyanato-B_{12r} has been evidenced and its main physicochemical features are described.

Being able to produce and monitor the interconversion of the three oxidation states of cobalt, electrochemistry has proved to be a valuable tool for investigating the electron-transfer steps and their coupling with ligand exchange reactions in the oxidoreduction chemistry of various vitamin B_{12} derivatives. It has, e.g., allowed a rather complete characterization of the B_{12a}–B_{12r}–B_{12s} system involving the determination of the main equilibrium thermodynamic parameters as well as the kinetic analysis of the oxidoreduction mechanisms.[2] A similar approach should be possible for cyanocobalamin as well. A first motivation for undertaking such a study is that cyanocobalamin is not only the most common form under which cobalamin is extracted from living organisms and dispensed in medical treatments, but also appears to be present per se in mammalian tissues and fluids[3a] and possibly involved in cyanide metabolism as suggested by several pathophysiological observations.[3]

A second, and more directly chemical, point of interest regards the thermodynamic and kinetic reactivity of Co(II) in the presence of cyanide. Under the influence of such a strong ligand the stabilization of the Co(III) forms as compared to the Co(II) forms could be such as to render the latter unstable toward disproportionation into Co(III) and Co(I):

$$2Co^{II} + 2CN^- \rightleftarrows Co^{III}(CN^-)_2 + Co^{I}$$
(equilibrium constant: K_D)

In other words, the standard potential of the Co(III)/Co(II) redox couple would then be close or even negative to that of the Co(II)/Co(I) couple, making the Co(III)/Co(I) oxidoreduction a direct two-electron process in equilibrium conditions. With a weak axial ligand such as water, disproportionation lies far to the left ($K_D \simeq 10^{-13}$).[1b] The replacement of H_2O by OH^- results in an increased tendency toward disproportionation even though, at pH 12, the constant remains very small ($\simeq 10^{-10}$).[1b] The question of the influence of an even stronger ligand, CN^-, on the disproportionation equilibrium is thus open to investigation. Let us now consider the generation of Co(II) species under nonequilibrium conditions, i.e., with a finite flux of electrons flowing. Their lifetimes and even the very existence of a cyanatocobalt(II) complex are, within the above thermodynamic framework, under the dependence of kinetic factors such as reduction rate of the Co(III) complexes, rate of the chemical evolution of the Co(II) species, and reduction rate of the Co(II) complexes themselves, which may all be functions of the cyanide concentration. While axial coordination of cob(III)alamin and cob(III)inamide by CN^- is now a well-documented topic,[4] very few data are available concerning the binding of cyanide on Co(II). To our knowledge, the only existing result is the ESR observation that CN^- weakly binds to cob(II)inamide.[5]

All the previous electrochemical studies of cyano- and dicyanocobalamin and cobinamide are reminiscent of the problems discussed above. Most of them were carried out in aqueous media with mercury as electrode material. The polarograms of cyanocobalamin,[6] dicyanocobalamin, and dicyanocobinamide[6a] exhibit a two-electron wave corresponding to the direct formation of B_{12s}. This is also apparent in cyclic voltammetry and the reoxidation wave of B_{12s} into B_{12r} is observed upon scan reversal.[7] The shape of the voltammograms indicates that the rate-controlling electron-transfer step is slow and probably affected by interfacial phenomena. The latter are likely to be at the origin of the difference observed between the half-wave potentials of dicyanocobalamin and dicyanocobinamide.[6b] These two compounds are indeed very similar as far as ligand binding forces and electron affinity are concerned. They essentially differ by their total charge: the cobinamide bears no net charge whereas the cobalamin has an additional −1 charge located on the phosphate group of the nucleotide side chain.

The observation of an apparently direct two-electron process in the polarographic and voltammetric reduction of cyanocobalamins does not necessarily imply that Co(II) is thermodynamically unstable toward disproportionation in the presence of cyanide. It has indeed already been observed in the case of hydroxobalamin that stability toward disproportionation may well coexist with an apparently direct two-electron voltammetric reduction which is then essentially related to the slowness of the initial electron-transfer step.[2b,c] This problem has also been investigated in the case of cyano- and dicyanocobalamins using a spectroelectrochemical technique with exhaustive electrolysis in a thin-layer cell.[8] It was thus shown that Co(II) indeed appears upon cathodic reduction of the cyanocobalamins before being reduced into B_{12s} at more negative potentials. Unfortunately, these experiments did not allow the assignment of the characteristic standard potential values owing to hysteresis between the reduction and the reoxidation pathways. The origin of this hysteresis phenomenon that might be related to the use of mercury as cathode material is not known with certainty.

It therefore appears that, owing to these various difficulties, very little is known so far about the reduction of cobalamin under the influence of cyanide both from the thermodynamic and mechanistic point of view. The work reported hereafter was an attempt to overcome these difficulties and to provide a thermodynamic characterization of the system as well as a description of the reaction pathways actually followed as a function of cyanide concentration, potential range, and time

0002-7863/80/1502-2654$01.00/0

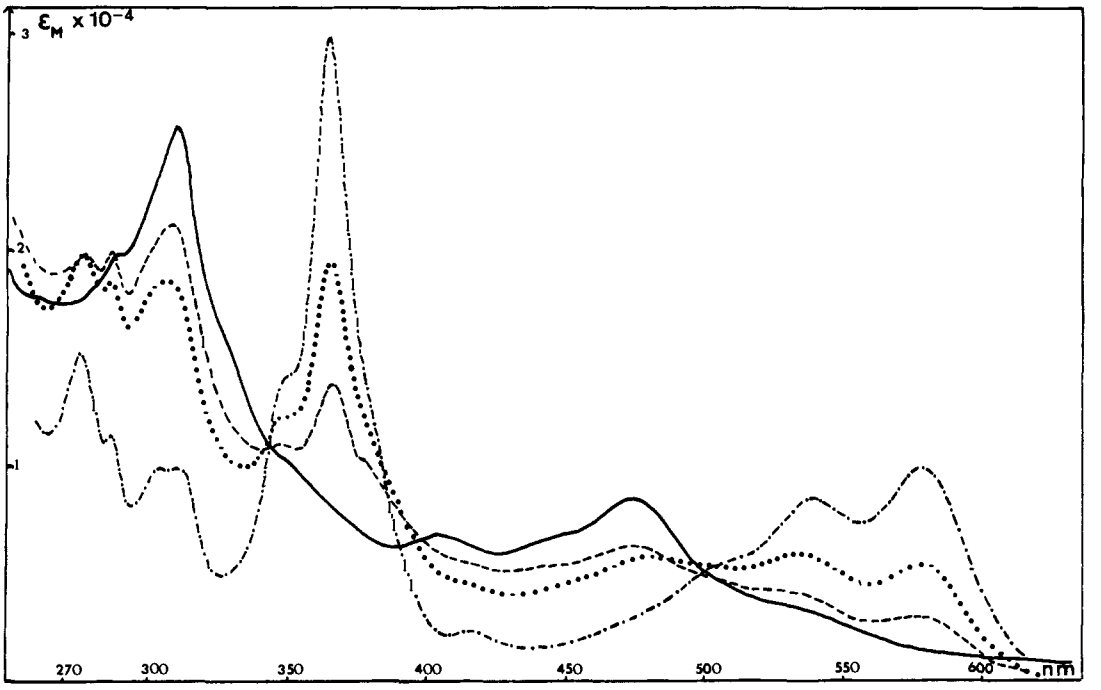

Figure 1. Spectrometric observation of the disproportionation of cob(II)alamin in the presence of 0.2 M KCN in an aqueous solution: (a) —, Co(II) before addition of CN^-; (b) ····· and - - - - -, evolution of the spectrum upon addition of CN^-; (c) - · -, after total oxidation.

scale. In this context, the case of cyanide is intended to represent a typical example of a more general problem, i.e., the interference of a strong ligand into the oxidoreduction pattern of cobalamins.

Redox Equilibrium Thermodynamics of Cobalamin in the Presence of Cyanide

The following experiment was carried out to test the *ability of cob(II)alamin to disproportionate in the presence of cyanide.* A 3×10^{-4} M solution of B_{12r} was prepared by exhaustive electrolysis of an aqueous solution of acetatocobalamin containing 1 M Na_2SO_4 in a conventional coulometric cell. It was then transferred under argon in the spectrometric cell. A KCN solution was then injected under argon into the cell so as to obtain a final CN^- concentration of $\simeq$0.2 M. The evolution of the spectrum with time was as shown in Figure 1. Co(I) clearly appears after mixing, together with the dicyanocobalamin. $Co^{III}(CN^-)_2$ is characterized by its bands at 368 and 580 nm while Co(I) is apparent through its band at 390 nm which gives rise to a shoulder on the side of the $Co^{III}(CN^-)_2$ Soret band.[4a] The initial Co(II) progressively disappears while Co(I) passes through a maximum and $Co^{III}(CN^-)_2$ increases continuously. This reflects the disproportionation of Co(II) into $Co^{III}(CN^-)_2$ and Co(I). The latter species is progressively consumed by trace oxygen which drives the reaction toward the complete conversion of the mixture into $Co^{III}(CN^-)_2$. This experiment clearly shows that Co(II) disproportionates to an appreciable extent in the presence of cyanide. The value of the maximal Co(I) concentration provides a lower estimation of the amount of Co(I) and $Co^{III}(CN^-)_2$ that would have been formed in the complete absence of oxygen. The maximal value of the Co(I) molar fraction is derived from the following equations representing the absorbance at 382 and 580 nm, i.e., at the most characteristic wavelengths of Co(I) and $Co^{III}(CN^-)_2$, respectively:

λ 382 nm:

$$1.34x_{Co(III)(CN^-)_2} + 0.74x_{Co(II)} + 2.74x_{Co(I)} = 1.42$$

λ 580 nm:

$$1.04x_{Co(III)(CN^-)_2} + 0.21x_{Co(II)} + 0.23x_{Co(I)} = 0.54$$

The coefficients represent the absorbances of each of the three species assuming that if $Co^{II}(CN^-)$ is formed its ϵ values are not very different from those of B_{12r} at these two wavelengths. The eventual error resulting from this approximation is certainly small since Co(II) absorption at these two wavelengths is weak as compared to one of the two other species. It is thus found that $x_{Co(I)} = 0.22$ and therefore that $K_D \geq 0.15$. Very similar results were found in another medium: 4:5 Me_2SO-1-propanol containing 0.1 M Bu_4-CN. It was then estimated that $K_D \geq 0.10$.

It is noted in Figure 1b that the spectrum of Co(II) in the presence of 0.2 M CN^- is slightly different from that of pure B_{12r} (Figure 1a), although an accurate comparison is made difficult by the fact that during the recording of the first spectrum some Co(I) and $Co^{III}(CN^-)_2$ have already been formed. The main visible difference is that the shoulder at 410 nm is more pronounced in the presence of CN^-, having then almost the shape of a band. This is what is expected for the effect of a strong ligand on the spectrum of B_{12r}. It has been indeed observed that the shoulder at 410 nm is enhanced when passing from the base-off to the base-on Co(II).[9a]

All this would point toward the conclusion that the Co(II) in the presence of 0.2 M CN^- exists under the form of a cyanato complex where the cyanide has replaced the 5,6-dimethylbenzimidazole as axial ligand. This is convincingly confirmed by the result of an *ESR investigation of the effect of CN^- on Co(II).* Electrolytically prepared B_{12r} was transferred into the ESR cell and CN^- injected along a procedure very similar to that described above in the case of UV-visible spectroscopy. The 4:5 Me_2SO-propanol mixture was used as solvent and 0.1 M Bu_4NCN was introduced into the cell. The lifetime of Co(II) was long enough to obtain before freezing a sufficient concentration for recording of the ESR spectrum. Figure 2 shows the comparison between the spectra recorded in the absence and in the presence of cyanide. The formation of the cyanato complex is clearly evidenced by the disappearance of the superhyperfine structure due to coupling with the benzimidazole nitrogen. Since the solution was freezed rapidly to prevent disproportionation, a small amount of base-on B_{12r} remains visible on the spectrum. The parallel hyperfine constant of Co passes from 105.6 to 80 G upon addition of CN^-,

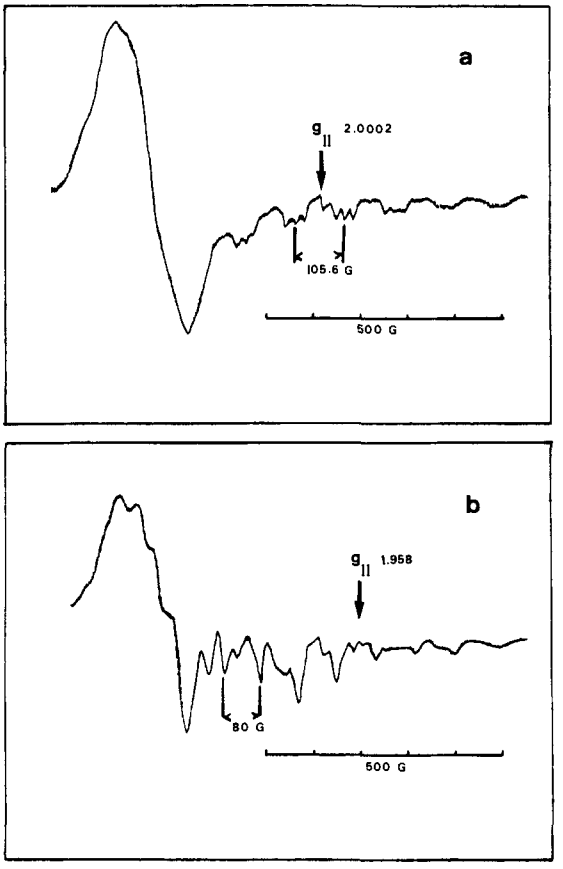

Figure 2. ESR spectra of B_{12r} in the absence of CN^- (a) and the presence of 0.1 M Bu_4NCN (b). Solvent: 4:5 Me_2SO–1 propanol. Temperature: 77 K.

which is in agreement with what was found for cyanocob(II)inamide.[5]

In order to obtain more quantitative data on the thermodynamics of the Co(III)-Co(II)-Co(I) system in the presence of CN^- a *spectroelectrochemical investigation* was carried out at two cyanide concentrations (0.1 and 0.01 M) and also with cyanocobalamin without cyanide addition, according to the same procedure as already employed for the B_{12a}-B_{12r} system.[2b] Au and Pt grid electrodes were found to give identical results. As pointed out previously, electron transfer to cyano- and dicyanocobalamin is expected to be slow. The equilibration duration at each potential was indeed found to be on the order of 1 h, which makes the recording of a whole spectrovoltammogram last several days.[10] No significant hysteresis between the reduction and the reoxidation scannings was observed.[10] A typical example of spectroelectrochemical analysis is shown in Figure 3 corresponding to the reduction of a 0.72×10^{-3} M solution of cyanocobalamin in water in the presence of 0.1 M KCN. The evolution of the spectrum as the potential is made more and more negative shows the conversion of Co(III) into Co(II) and then Co(I). It is apparent that there is no potential range where pure Co(II) can be obtained in accordance with the disproportionation tendency previously observed. Accordingly, differently located isosbestic points are observed at the edges of the potential range with no isosbestic points in the central region. The spectrovoltammograms obtained at 474 nm, i.e., a wavelength most characteristic of Co(II), are shown in Figure 4 for $[CN^-] = 0.1$ and 0.01 M.

The characteristic standard potentials for the Co(III)/Co(II) and Co(II)/Co(I) redox couples were derived from these spectrovoltammograms as follows. For $[CN^-] = 0.1$ and 0.01 M, Co(III) is present in the solution entirely under the form of dicyanocobalamin (the cyanation constant of cyanocobalamin is 6.3×10^3 in water[9a,b]). For $[CN^-] = 0.1$ M, Co(II) is entirely under its cyanato form. The optical absorbance can thus be expressed as

$$A = [A_1 \exp\{f(E - E_1^{0.1})\} \exp\{f(E - E_2^{0.1})\} + A_2 \exp\{f(E - E_2^{0.1})\} + A_3]/[\exp\{f(E - E_1^{0.1})\} \exp\{f(E - E_2^{0.1})\} + \exp\{f(E - E_2^{0.1})\} + 1]$$

where E is the electrode potential, $E_1^{0.1}$ and $E_2^{0.1}$ are the standard potentials of the Co(III)/Co(II) and Co(II)/Co(I) couples, $f = F/RT$, A is the observed absorbance, and A_1, A_2,

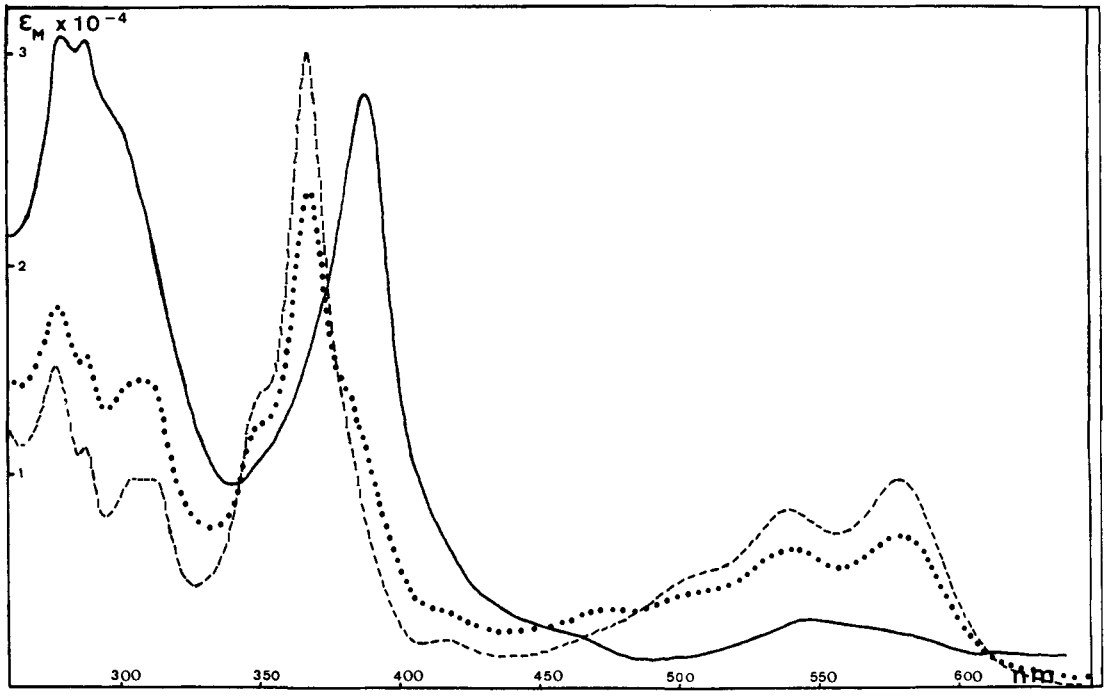

Figure 3. Spectroscopic analysis of the equilibrium reduction of cyanocobalamin (7.2×10^{-4} M) in water + 0.1 M KCN + 1 M Na_2SO_4 at an Au minigrid electrode. Equilibrium spectra at E: −0.75 (- - -); −0.95 (· · ·); −1.10 (—).

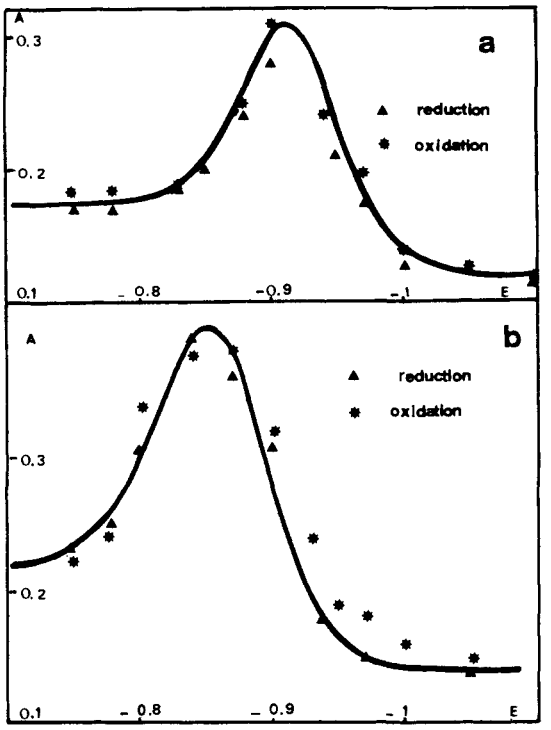

Figure 4. Spectrovoltammograms at 478 nm of the oxidoreduction of cyanocobalamin in the presence of cyanide in water + 1 M Na_2SO_4 at a Pt electrode: (a) KCN 0.1 M, B_{12} concn 7.2×10^{-4} M; (b) KCN 0.01 M, B_{12} concn 8.5×10^{-4} M. Solid lines: simulation of the experimental data (see text).

and A_3 are the absorbances of pure solutions of $Co^{III}(CN^-)_2$, $Co^{II}(CN^-)$, and Co(I), respectively, at the same concentration. A_1 and A_3 are known, while A_2, although probably close to the absorbance of the noncyanated base-on Co(II), is not. The above equation can be rewritten:

$$A_2 = a \exp(-fE_1^{0.1}) + b \exp(fE_2^{0.1}) + c$$

with

$$a = (A - A_1) \exp(fE),\ b = (A - A_3) \exp(-fE),\ c = A$$

There is one such equation for each value of the electrode potential. Average values of A_2, $E_1^{0.1}$, and $E_2^{0.1}$ are then derived from the resolution of this linear equation system. A_2, and thus $\epsilon^{478}_{Co(II)(CN^-)}$, is found to be 98% of the corresponding values for B_{12r} at the same wavelength. $E_1^{0.1}$ and $E_2^{0.1}$ are found to be close to −0.90 and −0.93 V, which will be taken as starting values for a more accurate fitting of the experimental data obtained both with 0.1 and 0.01 M CN^-. Combining the above $E_2^{0.1}$ value with the previously determined value of the $E°$ of the B_{12r}-B_{12s} couple[2a] (−0.850 V), the cyanation constant of B_{12r} is found as approximately equal to $K_A^{II} = 2 \times 10^2\ M^{-1}$. This shows that for $[CN^-] = 0.01$ M one has to consider the simultaneous presence of four species in the solution: $Co^{III}(CN^-)_2$, $Co^{II}(CN^-)$, Co(II), and Co(I). The optical absorbance is then given by the equation

$$A = [A_1 \exp\{f(E - E_1^{0.01})\} \exp\{f(E - E_2^{0.01})\} + A_2 K_A^{II} \exp\{f(E - E_2^{0.01})\} + A_3 \exp\{f(E - E_2^{0.01})\} + A_4]/[\exp\{f(E - E_1^{0.01})\} \times \exp\{f(E - E_2^{0.01})\} + K_4^{II} \exp\{f(E - E_2^{0.01})\} \times \exp\{f(E - E_2^{0.01})\} + 1]$$

with A_1, A_2, A_3, and A_4 being the absorbances of the pure four above species and $E_1^{0.01}$ and $E_2^{0.01}$ the standard potentials of the Co(III)/Co(II) and Co(II)/Co(I) couples for $[CN^-] = 0.01$ M ($E_1^{0.01} = E_1^{0.1} + 0.0586$, $E_2^{0.01} = E_2^{0.1} + 0.0586$ V). The spectrovoltammograms obtained for $[CN^-] = 0.01$ M are thus simulated using the values obtained for $[CN^-] = 0.1$ M. $E_1^{0.1}$ and $E_2^{0.1}$ are then slightly varied in order to achieve the best fit of the data obtained both for $[CN^-] = 0.1$ M and $[CN^-] = 0.01$ M. This is reached (solid lines in Figures 4a and 4b) for $E_1^{0.1} = -0.900$ and $E_2^{0.1} = -0.932$ V. It could be estimated by trying other values in the fitting procedures that the error on these determination is about ±3 mV.

It was further tested if the values thus obtained are consistent with the results of a spectroanalysis of the electrolysis of cyanocobalamin without addition of cyanide. It is apparent (Figure 5) that during this electrolysis dicyanocobalamin is formed through reaction of cyanocobalamin on the cyanide formed by its own reduction. This, which was not noticed in previous spectroanalysis of B_{12} reduction,[8] ought to be taken into account in the treatment of data. It also appears that the

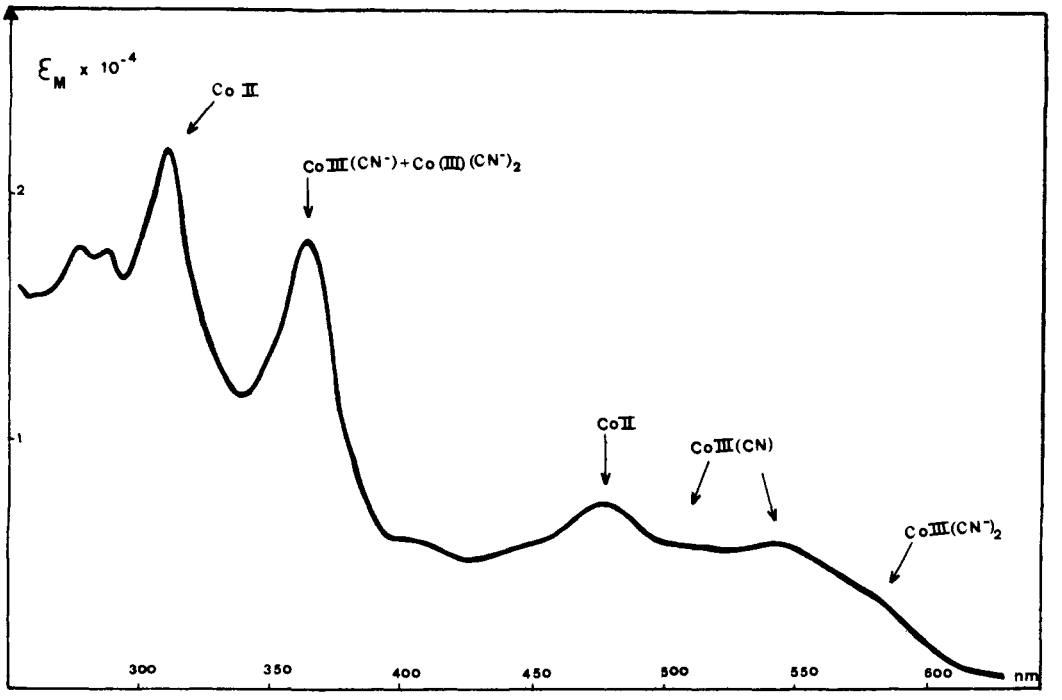

Figure 5. Spectrum of the equilibrium mixture obtained by electrolysis of cyanocobalamin (7.4×10^{-4} M) in water + Na_2SO_4 (1 M) at −0.65 V.

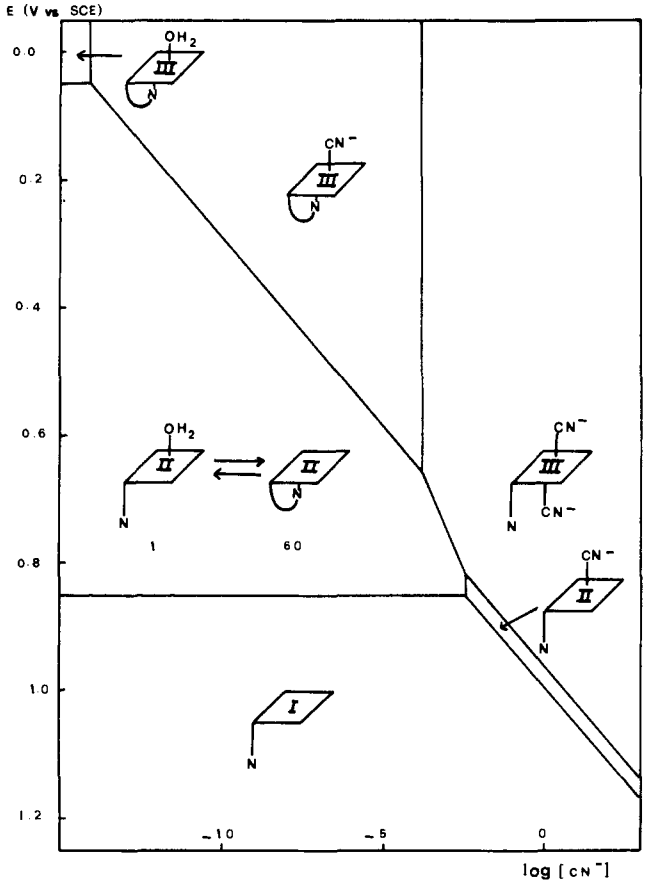

Figure 6. $E°$-log [CN^-] diagram in water.

reductions of Co(III) into Co(II) and of Co(II) into Co(I) occur within two fairly well separated potential ranges as noted previously.[8] The Co(III)/Co(II) oxidoreduction can be thus studied conveniently in the range −0.45 to −0.78 V. At any wavelength

$$(A_2 - A_1)x_2 + (A_3 - A_1)x_3 = A - A_1$$

where A is the observed optical absorbance, A_1, A_2, and A_3 are the absorbances of pure solutions at the same concentration of $Co^{III}(CN^-)_2$, $Co^{III}(CN^-)$, and Co(II), respectively, and x_2 and x_3 the molar fractions of $Co^{III}(CN^-)$ and Co(II).

Five such equations were considered at each potential for wavelengths most characteristic of Co(II) (312, 476 nm), $Co^{III}(CN^-)$ (548 nm), $Co^{III}(CN^-)_2$ (580 nm), and both $Co^{III}(CN^-)$ and $Co^{III}(CN^-)_2$ (360 nm). Averages values of x_2 and x_3 (and x_1, molar fraction of $Co^{III}(CN^-)_2$) were then derived from the resolution of this linear equation system at each potential, finally leading to the standard potential $E^{1.0}$ of the reaction:

$$Co^{III}(CN^-) + 1e \rightleftarrows Co(II) + CN^-$$

$$E^{1.0} = E - 0.0586 \log (x_2^2 K_A^{III}/x_1 x_3)$$

E being the applied potential and K_A^{III} the cyanation constant of cyanocobalamin. Taking $K_A^{III} = 6.3 \times 10^3$ M^{-1},[9] the following results were obtained:

E, V vs. SCE	x_1	x_2	x_3	$E^{1.0}$, V vs. SCE
−0.60	0.12	0.53	0.35	−0.871
−0.63	0.16	0.43	0.41	−0.879
−0.65	0.20	0.30	0.50	−0.870

The $E^{1.0}$ values thus found are in good agreement with the value −0.865, which can be derived from the $E_1^{0.1}$ and $E_2^{0.1}$ values obtained from the experiments with 0.1 and 0.01 M CN^- solution.

An $E°$-*log* [CN^-] *diagram* can finally be constructed from the above data, showing the ranges of thermodynamic stabilities of the various species as a function of the potential and the cyanide concentration (Figure 6).

It is noteworthy that the domain of stability of the cyanatocobalt(II) complex is extremely narrow, which confirms its tendency to disproportionate. The disproportionation equilibrium constant is indeed found to be $K_D = 0.28$.

Another important result is the value of the constant for the replacement of the 5,6-dimethylbenzimidazole of the nucleotide side chain by cyanide in the case of Co(II): $K_A^{II} = 2.4 \times 10^2$ M^{-1}. Using the $E°$ value previously determined for the B_{12a}/B_{12r} couple,[2b] the formation constant of cyanocobalamin from aquocobalamin is found to be equal to $10^{14.1}$ M^{-1}, which is in agreement with the previous determination[9b,d] ($K \geq 10^{12}$ M^{-1}).

An attempt was made to carry out similar experiments in the 4:5 Me_2SO-1-propanol mixture, which was the main reaction medium in the mechanism study.

The equilibrium constant for the conversion of cyanocobalamin was determined spectrophotometrically,[9a] without difficulty, starting from a 5×10^{-4} M solution of cyanocobalamin and adding small concentrations of Bu_4NCN in the range 10^{-5} to 5×10^{-2} M. It was thus found that $K_A^{III} = 10^4$ M^{-1}. However, meaningful data were found difficult to derive from the spectroelectrochemical experiments for the following reasons. Upon long time range reduction of $Co^{III}(CN^-)_2$ (the concentration of CN^- was 0.1 M) into Co(I) and reoxidation, an irreversible change of the spectrum was observed with new bands appearing at 486, 460, and 256 nm. This is presumably related to a modification of the ring resembling what occurs when yellow corrinoids are formed.[11] Although this phenomenon is slow, it prevents an accurate check of the reversibility of the oxidoreduction and thus a sound assessment of the $E°$-log [CN^-] diagram. The disproportionation constant seems somewhat higher than in water but it could not be determined with accuracy owing to the aforementioned phenomenon and also because the amount of Co(II) appearing upon reduction, although clearly visible, was found to be very small. It follows that the cyanation constant of B_{12r} could not be determined either. It is, however, probably not very different from that found in water. It is expected to be slightly larger as is actually K_A^{III}, owing to CN^- being less solvated and therefore more active in Me_2SO-propanol than in water.

Mechanisms

The kinetics of the oxidoreduction pathways of the B_{12}-cyanide system were studied by cyclic voltammetry mainly as a function of two parameters: the cyanide concentration and the sweep rate (v). Most of the experiments were carried out in the 4:5 Me_2SO-1-propanol mixture, which was found suitable in order to suppress the absorption and autoinhibition effects found in water when using a mercury working electrode. The use of this mixture was initially suggested by analogous observations made on the B_{12r}-B_{12s} system,[12] the Me_2SO-propanol mixture playing thus a similar role as the introduction of a large amount of tetrabutylammonium salt in the water solutions.[2a]

The use of a mercury electrode allows the observation of the reduction of the complexes of Co(III) with CN^-, as well as the reoxidation of the Co(I). It has, however, the disadvantage that the reoxidation waves of Co(II) are not observable, being obscured by the cyanide-assisted oxidation of mercury. This is the reason why a few experiments were carried out using a glassy carbon electrode in the same reaction medium.

Typical results obtained in these conditions are shown in Figure 7 which represents the evolution of the cyclic voltammograms at low sweep rates. The shape, height, and location

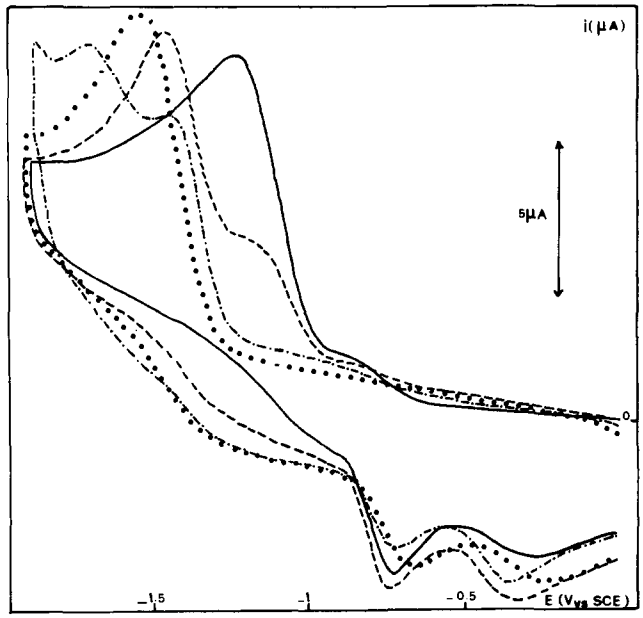

Figure 7. Cyclic voltammetry of cyanocobalamin on glassy carbon with successive addition of Bu_4NCN in 4:5 Me_2SO–propanol at 0.2 V s^{-1}, B_{12} concn 10^{-3} M. NBu_4CN concn: (1) 0, (2) 10^{-3}, (3) 2×10^{-3}, (4) 10^{-1} M. Supporting electrolyte: 0.1 M NBu_4BF_4.

of the peak were somewhat irreproducible and dependent upon the polishing of the electrode. Qualitatively, however, the following trends are clearly apparent. Upon addition of small amounts of cyanide the two-electron cathodic wave first decreases with simultaneous development of a second wave at a more negative potential, the total height remaining the same. The first wave then completely disappears at the expense of the second. Addition of larger amounts of CN^- further gives rise to another splitting of the wave with decrease of the first wave and appearance of a new wave at more negative potentials. Two waves are present on the anodic portion of the cyclic voltammogram. The most negative of these is located in a potential region corresponding to the reoxidation of Co(I) into Co(II). The other anodic wave has a peak located around −0.4 to −0.5 V vs. SCE. It features the reoxidation of Co(II) into Co(III). It is considerably (~500 mV) more negative that the reoxidation wave of B_{12r} into B_{12a}. (The standard potential of the B_{12a}–B_{12r} couple is approximately 0.02 V vs. SCE in 4:5 Me_2SO–propanol.[12]) Since the electron transfer from the Co(II) species is obviously a slow process as it is in the case for B_{12r},[2c] the only possible explanation of the effect of cyanide is that the Co(II) complex which undergoes oxidation is the cyanato complex, even though it is not in excess over B_{12r} at equilibrium:

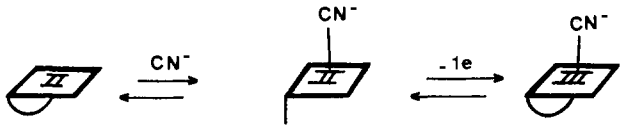

This implies that the cyanato complex is easier to oxidize than base-on B_{12r}, which is itself easier to oxidize than base-off B_{12r}[2c] in accordance with CN^- being a more electron-donating ligand than 5,6-dimethylbenzimidazole, which is itself more donating than the solvent (Me_2SO). Even without purposely added cyanide, the concentration of CN^- generated in the vicinity of the electrode during the cathodic scan is such, $\sim 10^{-3}$ M, that the $[Co^{II}CN^-]/[Co(II)]$ ratio is not exceedingly small. It is estimated to be in these conditions on the order of 0.2 on the basis of the K_A^{II} value previously determined. On the other hand, the cyanation and decyanation of Co(II) are rather fast processes, as will be seen later on. It is therefore perfectly

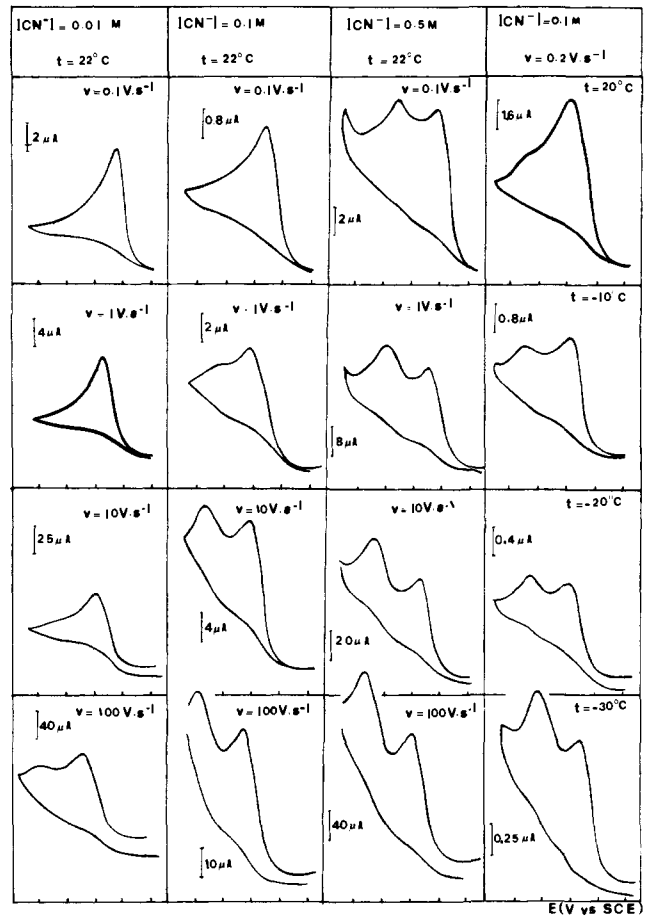

Figure 8. Reduction waves of cyanocobalamin in the presence of CN^- as a function of CN^- concn, sweep rate, and temperature. B_{12} concn: 4.5×10^{-3} M. Supporting electrolyte: 0.1 M NBu_4BF_4.

conceivable that oxidation of Co(II) will pass entirely through electron transfer from the cyanato complex without direct electron uptake from base-on and base-off B_{12r}.

Let us now examine the cathodic waves obtained on a mercury electrode. The general trends shown upon addition of CN^- are the same as for glassy carbon. However, the cyclic voltammograms are now quite reproducible and it is possible to investigate the effect of sweep rate.

For relatively *high CN^- concentrations*, i.e., above 5×10^{-3} M, the evolution of the voltammogram as a function of $[CN^-]$, sweep rate, and temperature is as follows (Figure 8). At room temperature, at the lower extremity of the CN^- concentration range, e.g., at 10^{-2} M, and for low sweep rates a single two-electron wave is observed. Upon raising the sweep rate and/or the CN^- concentration the height of this wave decreases and a new, more negative wave appears, the sum of the two remaining approximately constant. The maximal splitting is reached at 50 V s^{-1} for $[CN^-] = 0.5$ M. A further increase of the sweep rate does not modify the ratio of the two waves significantly. Their heights are then approximately equal, indicating that the reduction process is thus a succession of two one-electron steps. The same tendency of passing from a single two-electron wave to two successive one-electron waves is also observed, at given sweep rate and $[CN^-]$, upon decreasing the temperature (Figure 8).

That these two one-electron waves correspond to a stepwise reduction of Co(III) into Co(II) and then Co(I) is demonstrated by the experiment shown in Figure 9: when the cathodic scan is reversed beyond the second wave, the reoxidation peak of Co(I) is visible on the anodic trace; when it is reversed just after the first cathodic peak, Co(I) does not appear anymore on the anodic trace.

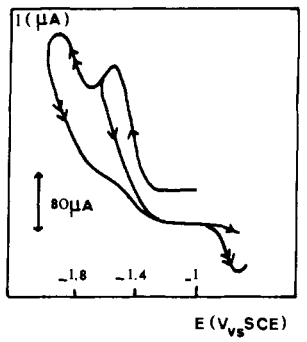

Figure 9. Cyclic voltammetry of cyanocobalamin on mercury in the presence of 0.1 M CN^- in 4:5 Me_2SO–propanol at room temperature. Sweep rate: 100 V s^{-1}. B_{12} concn: 1.58×10^{-3} M. Cathodic scan reversed at −1.55 (—→—) and −1.9 V (—→→—). Supporting electrolyte: 0.1 M NBu_4BF_4.

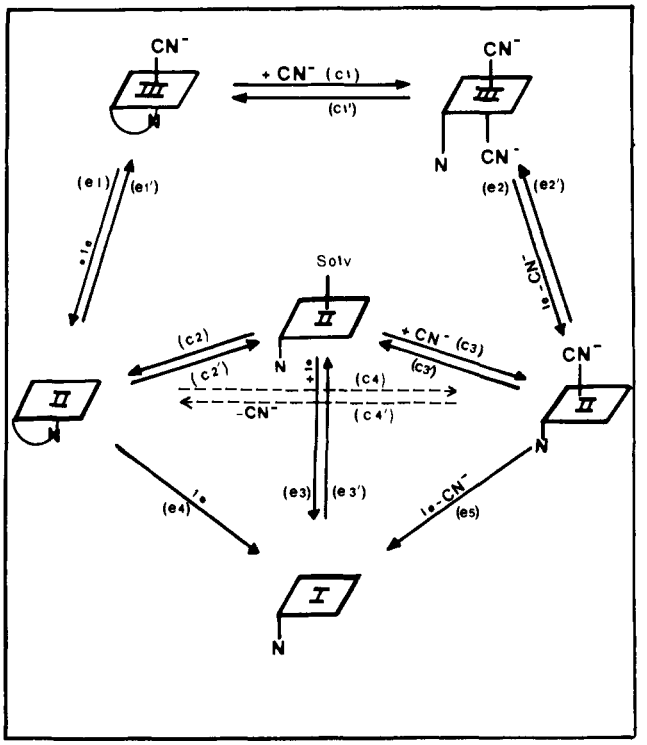

Figure 10. Mechanism chart.

The shift of the peak potential of both cathodic waves with sweep rate as well as their peak width is indicative of electrochemical processes controlled by the electron-transfer step. It is, however, noted that the transfer coefficient (~0.65) for the first wave is significantly larger than the usual value of 0.5.

All the above observations can be rationalized as follows (see the mechanism chart in Figure 10). Dicyanocob(III)alamin is the predominant Co(III) form in the considered CN^- concentration range and is therefore reduced directly (the influence of the interconversion $Co^{III}(CN^-)/Co^{III}(CN^-)_2$ on the reduction process will be discussed later on) by a one-electron transfer accompanied by CN^- cleavage into the cyanocob(II)alamin (step e2). The latter species then equilibrates with the base-off B_{12r} (steps c3 and c3′), which is immediately reduced into B_{12s} ($E^\circ = -0.78$ V[12]) at the potential of the first wave (step e3). The overall reaction thus follows an ECE mechanism,[13] leading to a total two-electron exchange at low sweep rate. Upon raising the sweep rate, step c3′ competes less and less favorably with the diffusion rate, which results in a progressive decrease of the first cathodic peak toward the value corresponding to a one-electron transfer. When this situation is reached, the cyanocob(II)alamin can be regarded as kinetically stable. The second wave thus features the reduction of the latter species into B_{12s} through a one-electron transfer accompanied by cyanide expulsion (e5). The height of the first wave is an increasing function of $[(k_3 + k_{3'})RT/Fv]^{1/2}/K_3$. ($K_3 = [Co^{II}CN^-]/[Co^{II}solv]$ at equilibrium.)[13] It follows that raising the sweep rate or the cyanide concentration, or decreasing the temperature, results in a lowering of the first wave at the expense of the second as observed experimentally (Figure 8).

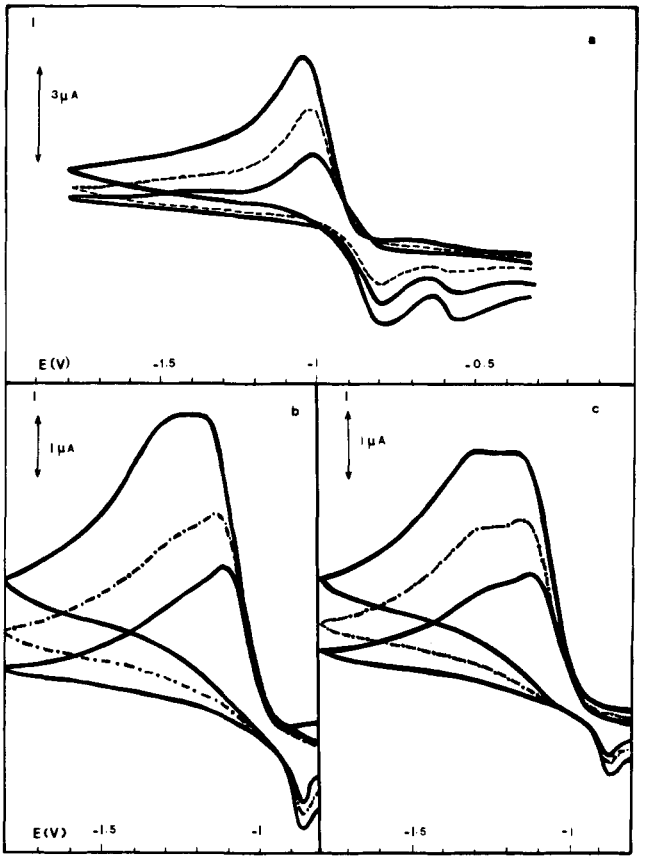

Figure 11. Cyclic voltammetry of cyanocobalamin on mercury in 4:5 Me_2SO–propanol without added CN^- as a function of temperature: 30.5 (a), −11 (b), −21 °C (c). Sweep rate: 0.05, 0.10, 0.20 V s^{-1} from the bottom upward. B_{12} concn: 1.6×10^{-3} M. Supporting electrolyte: 0.1 M NBu_4BF_4.

It is not possible to completely exclude a partial involvement of the (c4′ + e4) or (c3 + c2 + e4) pathways in the ECE process since base-on B_{12r} is also reduced (peak potential at, e.g., 0.1 V s^{-1}: −1.12 V) at the potential of the first wave. Since the base-off pathway is energetically more favorable, the involvement of the base-off form, if any, will tend to interfere upon raising the sweep rate. In the context of the above ECE mechanism, the second electron transfer is meant to occur at the electrode and not in the solution according to a disproportionation mechanism.[13] It has indeed already been noted that the disproportionation of Co(II) in the presence of cyanide occurs in at least several minutes, i.e., is much too slow to interfere within the time scale of cyclic voltammetry. A quantitative analysis of the kinetics of the ECE process by potential step chronoamperometry has been carried out. The results will be published elsewhere. However, a rapid estimation leads to a value of $k_{3'}$ on the order of 500 s^{-1}.

In the *absence of purposely added cyanide, cyanocobalamin* is also reduced along an ECE reaction sequence, involving, however, different steps than for dicyanocobalamin. At low and moderate sweep rates (Figure 11) a single two-electron cathodic wave is observed located at a less negative potential than for dicyanocobalamin (at, e.g., 0.1 V s^{-1} the peak potentials are −1.00 V for $Co^{III}CN^-$ and −1.33 V for

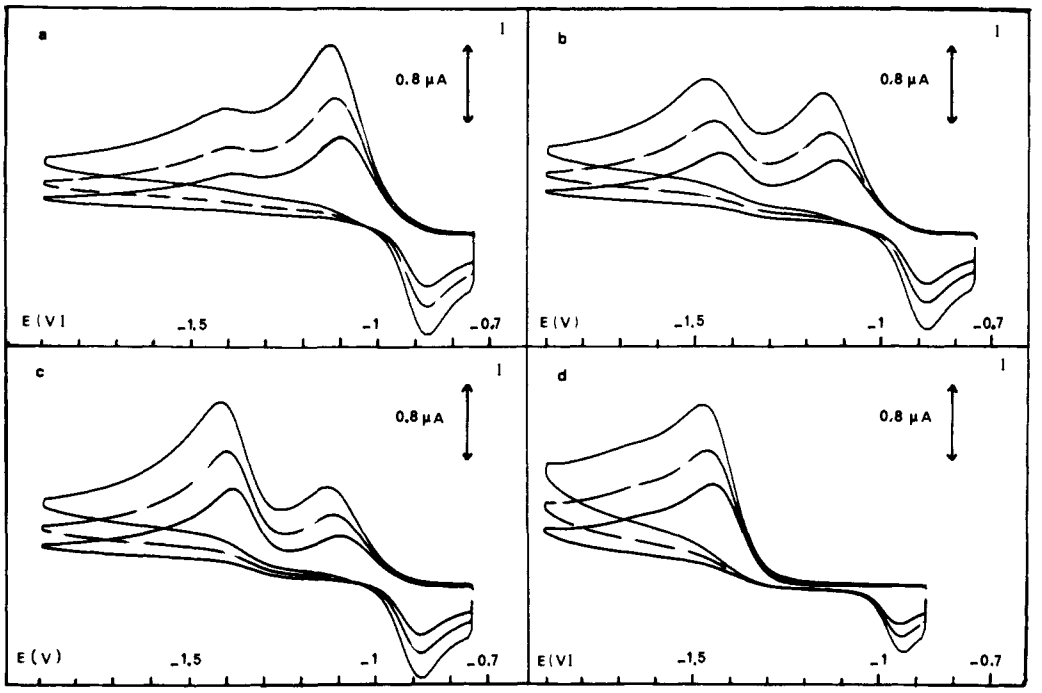

Figure 12. Cyclic voltammetry of cyanocobalamin on mercury in 4:5 Me_2SO–propanol in the presence of low concentrations of CN^-. CN^- concn: 10^{-3} (a), 2×10^{-3} (b), 4×10^{-3} (c), 5×10^{-3} mol L^{-1} (d). B_{12} concn: 1.58×10^{-3} (a), 0.45×10^{-3} M. (b, c, d). Sweep rate: 0.05, 0.10, 0.20 V s^{-1} from the bottom upward. Supporting electrolyte: 0.1 M NBu_4BF_4.

$Co^{III}(CN^-)_2$ at 22 °C). On the reverse scan the reoxidation wave of Co(I) into Co(II) is observed as well as another anodic wave at −0.55 V (for $v = 0.2$ V s^{-1}) featuring the cyanide-assisted oxidation of mercury. At very high sweep rates, i.e., above 100 V s^{-1}, a small second peak faintly appears in a potential region compatible with the reduction of base-on B_{12r}. It is more and more clearly observed upon decreasing temperature (Figure 11). At a given temperature it increases upon raising of the sweep rate. In water, the same behavior is observed as a function of temperature and sweep rate, the second peak appearing even more readily upon raising the sweep rate and lowering the temperature than in Me_2SO-propanol. All these observations suggest the following interpretation. At room temperature and for low and moderate sweep rates the e1c2′e3 pathway is followed. Base-off B_{12r} is indeed easier to reduce ($E^\circ = -0.78$ V[12]) than $Co^{III}CN^-$, while the opposite is true for base-on B_{12r} ($E_p = -1.12$ V at 0.1 V s^{-1} as compared to −1.00 V for $Co^{III}CN^-$ at the same sweep rate). On the other hand, the base-off/base-on equilibrium in 4:5 Me_2SO-propanol is not very much in favor of the base-on form ([base-on]/[base-off] $\simeq 2$[12] instead of 60 in water[2a]). This is the reason why the second peak featuring the reduction of base-on B_{12r} is so difficult to observe at room temperature. Upon lowering the temperature the equilibrium is more and more in favor of the base-on form and the reaction becomes slower and slower, which implies that lower and lower sweep rates are required for the second peak to appear as observed experimentally. The effect noted when passing from 4:5 Me_2SO-propanol to water also points to the same interpretation. The second peak then features the direct reduction of base-on B_{12r} into B_{12s} (step e4).

The above discussion also leads to the conclusion that any interference of the (c4′ + e4) or (c′3 + c′2 + e4) pathways in the reaction mechanism in the presence of added CN^- at room temperature would require very high sweep rates to be effective.

Turning back to the reduction of cyanocobalamin itself, it may be noticed that dicyanocobalamin is apparently not formed from the cyanide generated in the vicinity of the electrode upon reduction of the monocyano species in contrast to what was observed during the long time range spectroelectrochemical experiments. At 30 °C and very low sweep rates, however, a very small wave appears at the potential expected for dicyanocobalamin (Figure 11a). Concomitantly the CN^--assisted mercury oxidation wave slightly decreases. It was also observed that this dicyanocobalamin wave builds up upon repetitive scanning at low sweep rates. All this shows that dicyanocobalamin is actually formed by reaction of the electrogenerated CN^- on cyanocobalamin but that this is a slow process within the time scale of cyclic voltammetry.

This is confirmed by a series of experiments carried out at *low concentration of added* CN^- (Figure 12). Starting with a 5×10^{-4} M concentration of cyanocobalamin, the introduction of small amounts of Bu_4NCN results in a decrease of the $Co^{III}CN^-$ wave at the expense of a more negative wave featuring the reduction of $Co^{III}(CN^-)_2$. The ratio of the two waves is independent of sweep rate and its value for each CN^- concentration matches the ratio of the equilibrium concentrations of the two species as calculated from $K_A^{III} = 10^4$ M^{-1}. This shows that the conversion of cyanocobalamin into dicyanocobalamin is slow with respect to the time scale of cyclic voltammetry even at the lowest sweep rates. No detectable indirect reduction of dicyanocobalamin through the more reducible monocyanocobalamin occurs by kinetic displacement of the equilibrium. This is in agreement with a recent determination of the cyanation rate of B_{12} in water (2 M^{-1} s^{-1} at room temperature[14]). It explains why dicyanocobalamin is not detectably formed upon reduction of monocyanocobalamin within the time scale of cyclic voltammetry at room temperature as opposed to what was observed in spectroelectrochemical experiments which correspond to much longer electrolysis durations. One has to raise the temperature up to 30 °C or carry out repetitive cycles in order to detect a small second wave corresponding to dicyanocobalamin.

It is for the same type of reasons that there is no detectable influence of the base-off/base-on reaction on the reduction of cyanocobalamin within the time scale of cyclic voltammetry as opposed to what was observed for B_{12r}.[2a] This means that the equilibrium ratio of the base-off and base-on forms of cyanocobalamin is too small and the conversion of the base-on

into the base-off form too slow for an indirect reduction of the base-on form through the base-off form to be detected. Based on the data obtained in water[14] the ratio of indirect over direct reduction of the base-on species is indeed estimated[15] to be 10^{-3} at room temperature. Although the base-off form might be more favored in Me_2SO-propanol, it can be concluded from the present observation that the ratio of indirect over direct reduction is less than 1%.

An overall picture of the possible reaction pathways is given in Figure 10. The way in which the reaction pathway changes as a function of the two main external parameters, CN^- concentration and electron flux, can be summarized as follows.

As soon as the CN^- concentration is three to four times that of cyanocobalamin, the reduction starts from the dicyanocobalt(III) yielding in a first stage (e2) the cyanocobalt(II) with concomitant loss of a CN^- under electron transfer kinetic control. Two competitive pathways are then followed for the further reduction into Co(I): (c3′ + e3), which predominates at low CN^- concentration and low sweep rate giving rise to a two-electron ECE process; direct reduction of $Co^{II}CN^-$, which predominates at high CN^- concentration and high sweep rate and occurs when electron transfer kinetic control at a potential negative to (e2) giving rise to a separated one-electron wave. Starting from cyanocobalamin without addition of CN^-, the reaction pathway is (e1 + c2′ + e3), i.e., a two-electron ECE process which is under the kinetic control of the first electron transfer. High sweep rates and low temperatures are required to observed a detectable contribution of reaction (e4). When the CN^- concentration is comprised between zero and three times that of the starting cyanocobalamin, there is a competition between the two reaction pathways (e1 + c2′ + e3) and (e2 + c3′ + e3) on the basis of the equilibrium ratio of cyano- and dicyanocobalamin, the conversion rate of the second into the first being too slow to interfere into the reduction process. Starting from Co(I), the reoxidation process follows the (e3′ + c3) pathway, which appears as energetically favored even when the starting solution contains cyanocobalamin without CN^- added. In the presence of CN^-, $Co^{II}CN^-$ is then reoxidized into $Co^{III}(CN^-)_2$, while in the absence of added CN^-, $Co^{II}CN^-$ is reoxidized directly into cyanocobalamin (not represented in Figure 10).

Conclusion

A detailed description of the thermodynamic and mechanistic features of the oxidoreduction of vitamin B_{12} in the presence of cyanide has been given in the preceding sections. Let us, as a conclusion, emphasize some particularly important points.

The interaction of cyanide with cobalt atom results in a strong tendency toward direct two-electron reduction of Co(III) into Co(I). At equilibrium, the disproportionation constant reaches 0.28 as soon as the cyanide concentration is larger than 5×10^{-3} M. This is to be compared with the effect of OH^-: the disproportionation equilibrium constant is only 10^{-10} for $[OH^-] = 10^{-2}$ M. For the reduction of cyanocobalamin itself, although the two reduction steps are clearly separated, their distance in potential is rather small. Its exact value is dependent upon the initial B_{12} concentration; for, e.g., 10^{-3} M $\Delta E° = 178$ mV, which would correspond to a disproportionation constant of 10^{-3}. Although the two reduction steps are thermodynamically successive, from a kinetic point of view, cyanocobalamin is reduced along a two-electron process for electron fluxes as low as 10^{-6}–10^{-5} A/cm^2. This is because the electron transfer to Co(III) is a slow process while the reduction of the resulting B_{12r} through its base-off form is markedly more rapid. However, when adding sufficient amount of CN^-, the two reduction processes become successive again. This corresponds to the Co(II)/Co(I) reduction passing entirely through cyanocob(II)alamin to which electron transfer is much slower than to base-off B_{12r}. For a given CN^- concentration, this is the more pronounced the higher the flux of electrons flowing through the system. The problem of two successive one-electron vs. one single two-electron reduction steps would presumably present the same features for strong ligands other than CN^- such as those which may stand in the vicinity of the cobalt atom in enzymatic systems.

The existence of the cyanato B_{12r} has been clearly evidenced and its thermodynamic and kinetic features have been evaluated. The equivalent concentration of 5,6-dimethylbenzimidazole in the nucleotide side chain is at least 0.1 M. From this and the value of K_A^{II} it is then concluded that CN^- is intrinsically stronger a ligand toward Co(II) than 5,6-dimethylbenzimidazole.

Experimental Section

Cells, electrodes, and instrumentation were the same as previously described for cyclic voltammetry[2a] as well as for spectroelectrochemistry.[2b] The UV–visible spectrometer was a Cary-Varian 219. The ESR spectrometer was a Varian (V 4502) X-band. The reference electrode was an aqueous saturated calomel electrode in water as well as in the Me_2SO–propanol mixture.

Chemicals. Me_2SO (Uvasol grade) and 1-propanol (proanalysis) were obtained from Merck, Bu_4NCN (purissimo) from Fluka, and cyanocobalamin from the Rhone-Poulenc Co. They were used as received.

Acknowledgment. The work was supported in part by the CNRS (Equipe de Recherche Associée 309 "Electrochimie Moléculaire"). We thank Mrs. Jomain for helpful technical assistance in the spectroelectrochemical experiments. We are grateful to Drs. J. M. Lhoste and J. Mispelter (Fondation Curie-Institut du Radium, Section de Biologie) for the permission to use the ESR spectrometer and for helpful advice when carrying out the ESR experiments. We thank the Rhone-Poulenc Co. for the supply of vitamin B_{12} samples.

References and Notes

(1) (a) Laboratoire d'Electrochimie de l'Université de Paris VII. (b) Laboratoire de Biophysique du Muséum d'Histoire Naturelle.
(2) (a) Lexa, D.; Savéant, J. M. *J. Am. Chem. Soc.* **1976**, *98*, 2652. (b) Lexa, D.; Savéant, J. M.; Zickler, J. *Ibid.* **1977**, *99*, 2786. (c) De Tacconi, N. R.; Lexa, D.; Savéant, J. M. *Ibid.* **1979**, *101*, 467.
(3) (a) Linnell, J. C. In "Cobalamin, Biochemistry and Pathophysiology", Babior, B. M. Ed.; Wiley-Interscience: New York, 1975; pp 289–333. (b) Beck, W. S. In ref 3a.
(4) (a) Pratt, J. M. "Inorganic Chemistry of Vitamin B12"; Academic Press: New York, 1972. (b) Hogenkamp, H. P. C. In ref. 3a, pp 21–74.
(5) Bayston, J. H.; Looney, F. D.; Pilbrow, J. R.; Windfield, M. E. *Biochemistry* **1970**, *9*, 2164.
(6) (a) Jaselskis, B.; Diehl, H. *J. Am. Chem. Soc.* **1954**, *76*, 4346. (b) Hogenkamp, H. P. C.; Holmes, S. *Biochemistry* **1970**, *9*, 1886. (c) Kenyhercz, T. M.; Mark, H. B. *Anal. Lett.* **1974**, *7*, 1. (d) Abd-El-Nabey, B. A. *J. Electroanal. Chem.* **1974**, *53*, 317.
(7) (a) Tacket, S. L.; Ide, J. W. *J. Electroanal. Chem.* **1971**, *30*, 510. (b) Swetik, P. G.; Brown, D. G. *Ibid.* **1974**, *51*, 433. (c) Swetik, P. G.; Brown, D. G. *Biochim. Biophys. Acta* **1974**, *343*, 641.
(8) (a) Kenyhercz, T. M.; De Angelis, T. P.; Norris, B. J.; Heineman, W. R.; Mark, H. B. *J. Am. Chem. Soc.* **1976**, *98*, 2469. (b) Kenyhercz, T. M.; Mark, H. B. *J. Electrochem. Soc.* **1976**, *123*, 1656.
(9) (a) Cockler, S.; Hill, H. A. O.; Ridsdale, S.; Williams, J. P. *J. Chem. Soc., Dalton Trans.* **1971**, 297. (b) George, P.; Irvine, D. H.; Glauser, S. C. *Ann. N.Y. Acad. Sci.* **1960**, *88*, 393. (c) Firth, R. A.; Hill, H. A. O.; Pratt, J. M.; Thorp, R. G.; Williams, R. P. J. *J. Chem. Soc. A* **1968**, 2428. (d) Hayward, G.; Hill, H. A. O.; Pratt, J. M.; Vanston, N. J.; Williams, R. P. J. *J. Chem. Soc. A* **1965**, 6485.
(10) A Ni–Hg minigrid electrode prepared according to a previously described procedure[8] was also employed. It showed no significant hysteresis provided that one does not cross the potential values where cyanide-assisted oxidation of mercury occurs. It did not demonstrate significantly shorter equilibration durations than either Au or Pt. We found it, however, extremely difficult to get rid of residual amounts of mercuric ions generated through cyanide-assisted air oxidation of Hg and that can bind benzimidazole[4] as shown by a very large increase of absorbance in the benzimidazole region (288 nm) of the Co(III) spectra. Detachment of the nucleotide side chain under the influence of Hg^{2+} may then alter the conclusions of the analysis of the Co(III)/Co(II) system.

(11) Gossauer, A.; Grüming, B. Proceedings of the Third European Symposium on Vitamin B12 and Intrinsic Factor, Zurich, in press.
(12) Faure, D.; Lexa, D.; Savéant, J. M.; Zickler, J., unpublished results.
(13) (a) Mastragostino, M.; Nadjo, L.; Savéant, J. M. *Electrochim. Acta* **1968**, *13*, 721. (b) Amatore, C.; Savéant, J. M. *J. Electroanal. Chem.* **1977**, *85*, 27. (c) Amatore, C.; Savéant, J. M. *Ibid.*, in press.
(14) Reenstra, W. W., Jencks, W. P. *J. Am. Chem. Soc.* **1979**, *101*, 5780.
(15) Savéant, J. M.; Vianello, E. *Electrochim. Acta* **1963**, *12*, 905.

Synthesis and Spectroscopic and Structural Properties of Bis(*N*-acetyl-DL-tryptophanato)copper(II) Complex and Its Amine Adducts. Effect of Amines on the Amino Acid Coordination. Crystal and Molecular Structure of Diaquabis(*N*-acetyl-DL-tryptophanato)bis(pyridine)-copper(II)

L. P. Battaglia,[1a] A. Bonamartini Corradi,[1a] G. Marcotrigiano,[1b] L. Menabue,[1c] and G. C. Pellacani*[1c]

Contribution from the Consiglio Nazionale delle Ricerche of Italy, the Istituto di Chimica Generale, Centro di Studio per la Strutturistica Diffrattometrica del C.N.R., University of Parma, 43100 Parma, Italy, Istituto di Chimica, Facoltà di Medicina-Veterinaria, University of Bari, 70126 Bari, Italy, and Istituto di Chimica Generale e Inorganica, University of Modena, 41100 Modena, Italy. *Received May 29, 1979*

Abstract: A green compound of the type $Cu(Actrp)_2 \cdot H_2O$ (Actrp = *N*-acetyl-DL-tryptophanate ion) and its aromatic and aliphatic heterocyclic amine adducts, $Cu(Actrp)_2B_2$ (B = pyridine (py), 3- and 4-methylpyridine (3- and 4-pic), *N*-methylpiperazine (NCH_3pipz), morpholine (morph), and piperidine (pipd)), $Cu(Actrp)_2(py)_2(H_2O)_2$, and $Cu(Actrp)_2 \cdot$pipz (pipz = piperazine), were prepared and characterized by means of low- and room-temperature magnetic and EPR measurements and room-temperature electronic and infrared spectroscopy. While $Cu(Actrp)_2 \cdot H_2O$ shows physical properties indicating a binuclear configuration, all the aromatic heterocyclic amine adducts appear to possess a tetragonal configuration with CuO_4N_2 chromophore. For one of the latter complexes, diaquabis(*N*-acetyl-DL-tryptophanato)bis(pyridine)copper(II), the crystal structure was also determined by single-crystal X-ray diffraction methods. The complex crystallizes in the monoclinic space group $P2_1/c$ with two molecules in a unit cell of dimensions $a = 9.377$ (6) Å, $b = 19.341$ (14) Å, $c = 11.615$ (7) Å, $\beta = 123.2$ (2)°, $d_{calcd} = 1.41$ g cm^{-3}, $d_{measd} = 1.42$ g cm^{-3}. Least-squares refinement of the 150 variables has led to a value of the conventional R index (on F) of 0.071 for 783 independent reflections having $F > 4\sigma(F)$. The geometry about the copper atom, which is coordinated to two carboxylic oxygens and two pyridine nitrogen atoms, is completed to an elongated tetragonal bipyramid by two weak interactions with two water molecules. The Cu–N, Cu–O(amino acid), and Cu–O(water) distances are 1.95 (1), 2.02 (1), and 2.61 (1) Å, respectively, and the O(amino acid)–Cu–N angle is 87.9 (6)°. For the adducts of the aliphatic heterocyclic amines a square-planar geometry with CuO_2N_2 chromophore may be suggested. In all the complexes reported in this work the amino acid appears to coordinate the copper(II) ion only toward the carboxylate group. For the assignment of the way in which the carboxylate group coordinates, we suggest that the observation of the position of the $\nu(OCO)_s$ is particularly relevant.

Introduction

Coordination chemists have been interested for many years in the donor properties of amino acids as models for metal-protein interaction.

The amino acids containing terminal *N*-acetyl residues are of particular interest not only because they are present in some natural proteins and peptides, but also because it is possible that an acetyl amino acid might be the starting unit in the biosynthesis of some peptide chains which grow by the stepwise addition of amino acyl residues to the acetylated N-terminal amino acid.[2] In particular *N*-acetyl-DL-tryptophan inhibits complex formation between pepsin and bovine serum albumin and also stabilizes serum albumin against denaturation by heat, urea, and guanidine salts and against isomerization at pH 4.[3]

N-Acetyltryptophan was furthermore found as a metabolite excreted in the urine by normal and cancer patients before and after tryptophan feeding. In particular it was reported that *N*-acetyl-D-tryptophan ingestion by man did not increase the amount of these metabolites excreted, while acetyl-L-tryptophan ingestion raised the urinary excretion but less than that observed for equimolar quantities of L-tryptophan or D-tryptophan. Langner and Edmonds have also shown that acetyl-D-tryptophan is poorly adsorbed.[4]

Having paid particular attention to the coordination properties of *N*-acetyl and *N*-benzoyl amino acids,[5] we have investigated in this paper the coordination behavior of *N*-acetyl-DL-tryptophan (hereafter abbreviated as ActrpH) toward the copper(II) ion and the effect of amines on the amino acid coordination.

All the synthesized compounds were characterized by means of electronic, infrared, and EPR spectroscopy and magnetic moment measurements, and for one of them, the only one of which more suitable crystals, although very thin, were obtained, the crystal structure was also determined.

This work also takes on great interest from the fact that the metal-tryptophanate systems have generally been poorly examined[6] and till now the crystal structure of only one tryptophanate, the glycyl-L-tryptophanatocopper(II) trihydrate,[7,8] is known.

0002-7863/80/1502-2663$01.00/0